Kobe University Repository : Kernel

Create Date: 2017-12-19

PAPER

Fullband Simulation of Nano-Scale MOSFETs Based on a Non-equilibrium Green's Function Method

Helmy FITRIAWAN[†a)], *Nonmember*, Matsuto OGAWA[††], *Member*, Satofumi SOUMA[††], *Nonmember*, and Tanroku MIYOSHI[††], *Member*

SUMMARY The analysis of multiband quantum transport simulation in double-gate metal oxide semiconductor field effects transistors (DG-MOSFETs) is performed based on a non-equilibrium Green's function (NEGF) formalism coupled self-consistently with the Poisson equation. The empirical $sp^3 s^*$ tight binding approximation (TBA) with nearest neighbor coupling is employed to obtain a realistic multiband structure. The effects of non-parabolic bandstructure as well as anisotropic features of Si are studied and analyzed. As a result, it is found that the multiband simulation results on potential and current profiles show significant differences, especially in higher applied bias, from those of conventional effective mass model.
key words: non-equilibrium Green's function, quantum transport, tight-binding approximation, $sp^3 s^*$, double-gate MOSFETs, Poisson's equation

1. Introduction

As the size of current devices is scaling down into nanometer scale [1], atomistic simulations become necessary for an accurate modeling of their structural, electronic and transport properties. Such microscopic approaches are important in order to account correctly for quantum phenomena, i.e. atomic-scale fluctuations, local bond distortions, alloy effects, quantum tunneling effects and energy quantization, occuring in such devices. The effective mass approximation (EMA), where only the wavefunction envelope is considered inspite of the atomic details, may not be accurate anymore due to such quantum effects in nanostructures. Thus it motivates the use of more realistic full band structures in quantum transport simulations [2]–[4]. Quantum mechanical simulation with atomistic resolutions can be achieved using localized basis sets for the description of the system Hamiltonian. Semi-empirical tight-binding approach, a full band technique, proves extremely useful for the atomistic treatment of nanoscale devices with any materials, provided that the tight-binding parameters for the material are known in advance [5]–[7]. The energy-dispersion relation of full multiband structure is different, especially in higher energy far from the conduction band minimum, with that of EMA model [8], [9], which could give different quantum transport characteristics.

This paper reports the calculation of quantum electron transport in double-gate MOSFETs in which quantum effects are the highest concern [10]–[17]. The transport simulation is formulated based on non-equilibrium Green's function (NEGF) which provides a reliable theoretical basis for the development of atomic-level quantum mechanical simulators for nanoscale devices [18], [19]. In the next section, the theory of tight-binding model and the application of Green's function based on multiband tight-binding model will be discussed. In the formulation, the empirical $sp^3 s^*$ tight-binding approximation (TBA) model is employed to obtain more realistic full band structure [6], [7]. The NEGF method is performed self-consistently coupled with the Poisson equation to acquire the effect of space charge density in the calculation. Some numerical results on simulated devices are presented and compared with those of effective mass model in Sect. 3. Finally, our works are concluded in the last section.

2. Simulation Method

2.1 Tight-Binding Model

The calculation of quantum electron transport is constructed based on empirical TBA model to obtain more realistic band structure. The carrier transport is assumed to be confined in [100] direction in nano-scale quantum structures. In the model five atomic orbitals per atom (s, p_x, p_y, p_z and s^*) assuming nearest neighbour overlaps are taken into consideration. The basis set is assumed to be spatially localized.

In the tight binding scheme, the system Hamiltonian is represented by a basis set of atomic-like orbitals, $\left| k_\parallel, L, \alpha^b \right\rangle$, described by a site index, L, (which consist of one anion and one cation atoms) and a symmetry-related index, α^b (b = anion or cation), which specifies the angular momentum and spin index associated with the in-plane wave vector, $k_\parallel$ [5]. Therefore, the total electron wave function is expressed as a linear combination of the atomic orbitals (LCAO)

$$\left| \Psi(k_x, k_\parallel, x) \right\rangle = \sum_{L, \alpha^a, \alpha^c} \{ C_{L, \alpha^a(k_x)} \left| k_\parallel, L, \alpha^a \right\rangle + C_{L, \alpha^c(k_x)} \left| k_\parallel, L, \alpha^c \right\rangle \} \tag{1}$$

where k_x is a propagating wave vector.

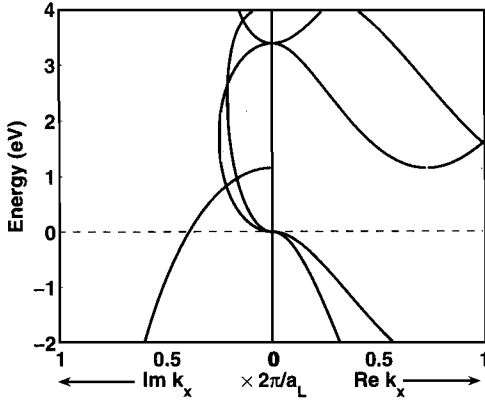The Schrödinger equation in the TBA basis may be written as

Fig. 1   Complex bandstructure of bulk silicon along the [100] direction. Re k_x shows the more realistic bandstructure of Si with indirect bandgap. The origin of the electron energy is located at the top of the valence band.

$$(H - E) \left| \Psi(k_x, k_\parallel, x) \right\rangle = 0 \tag{2}$$

where H is the system Hamiltonian and E is the electron energy. By projecting Eq. (2) on the atomic orbitals located at atomic layer l, we will have the following eigenvalue equation [20]–[22].

$$T_c T_a \begin{pmatrix} C_a \\ C_c \end{pmatrix} = \exp(-ik_x\Delta) \begin{pmatrix} C_a \\ C_c \end{pmatrix} \tag{3}$$

where T_c and T_a are defined by

$$T_b = \begin{bmatrix} -\left[H^b_{l,l-1}\right]^{-1} \left[H^b_{l,l}\right] & -\left[H^b_{l,l-1}\right]^{-1} \left[H^b_{l,l+1}\right] \\ 1 & 0 \end{bmatrix} \tag{4}$$

Δ is one monolayer spacing which is equal to one-half of material lattice constant and $H^b_{l,l}$, $H^b_{l,l-1}$ and $H^b_{l,l+1}$ are 5×5 matrices which define the onsite energies for cation ($b = c$) or anion ($b = a$) and hopping energies between the nearest atom. The elements of this matrix defined in terms of tight-binding parameters can be found in Refs. [6], [7], [23]. In the silicon crystal, the parameters for anion and cation atoms are equivalent.

This eigenvalue problem produces bloch states, where half of these states propagate or decay to the right while the the rest propagate to the left. The complex band structure for silicon, solved from Eq. (4), is plotted in Fig. 1.

2.2 Multiband Non-equilibrium Green's Function

For the analytical solution of quantum transport, we use a non-equilibrium Green's function (NEGF) method based on the multiband tight-binding model as described in the previous section. In the ballistic tranport simulation, the NEGF method is equivalent by means of solving the Schrödinger equation.

The retarded Green's function may be obtained from the following equation

$$G^R = \left[(E - i0^+)I - H - \Sigma_L - \Sigma_R\right]^{-1} \tag{5}$$

where E is the energy and the matrix elements of device

Hamiltonian along the transport direction may be written as

$$\left\langle \alpha, L, k_\parallel \middle| H \middle| \alpha', L', k'_\parallel \right\rangle = D_{\alpha,\alpha';L}(k_\parallel)\delta_{L,L'}$$
$$- t_{\alpha,L;\alpha',L'}(k_\parallel)\delta_{L,L\pm1} \tag{6}$$

H is a block tridiagonal matrix, $D_{\alpha,L}$ contains the orbital energies and the electrostatic potential, and $t_{\alpha,L;\alpha',L'}$ are the hopping energies between the two nearest layers. The boundary self-energy, $\Sigma_{L,R}$, which take into account the effect of semi-infinite left and right contacts into the device, can be calculated from

$$\Sigma_L = -t_{0,1}XKX^{-1} \tag{7}$$
$$\Sigma_R = -t_{N,N+1}XKX^{-1} \tag{8}$$

where the eigenvalues, K, and eigenvectors, X, are obtained by solving the eigenvalue equation of Eq. (4).

At the left and right end of the device, the boundary Green's function is found to be coupled with the bulk modes [20], [21]. We have used recursive Green's function algorithm as in Ref. [24] to calculate the retarded Green's function in the left and right contacts.

In order to calculate the carrier and current densities, we have to determine the lesser Green's function from the retarded Green's function.

$$-iG^<_{L,L} = \sum_{L_1,L_2} f_L G^R_{L,L_1}\Gamma^{BL}_{L_1,L_2}G^A_{L_2,L} + f_R G^R_{L,L_1}\Gamma^{BR}_{L_1,L_2}G^A_{L_2,L} \tag{9}$$

where f_L and f_R are the Fermi Dirac factors of the left and right contacts, respectively. Hence, we can calculate the carrier and current densities, respectively, from

$$n_L = \frac{-2i}{A\Delta} \sum_{k_\parallel} \int \frac{dE}{2\pi} tr\left\{G^<_{L,L}(k_\parallel, E)\right\} \tag{10}$$

$$J_L = \frac{2e}{\hbar A} \sum_{k_\parallel} \int \frac{dE}{2\pi} 2Re\left\{tr[t_{L_1;L_2}G^<_{L_2;L_1}(k_\parallel, E)]\right\} \tag{11}$$

where A is the cross sectional area of the device, e is the electronic charge and tr is a trace over the whole atomic orbitals. We have performed both Eqs. (10) and (11) for all subbands and all valleys to obtain total 3D carrier and current densities.

3. Results and Discussions

The calculation of quantum transport with multiband NEGF is performed to the double-gate (DG) MOSFET with device structure as shown in Fig. 2.

The device has an intrinsic channel and the source/drain is doped at $1 \times 10^{26} \text{ m}^{-3}$, respectively. It is assumed to have symmetrical gates which control the channel region. The channel is assumed to be Si with no gate-to-source/drain overlap. The junctions are modeled as abrupt. The oxide thickness is 1.0 nm for both top and bottom gates and the silicon thickness is 3.0 nm. Two types of valleys, two- and four-fold valleys, are taken into the consideration. The two-fold valleys have heavier effective mass while the four fold
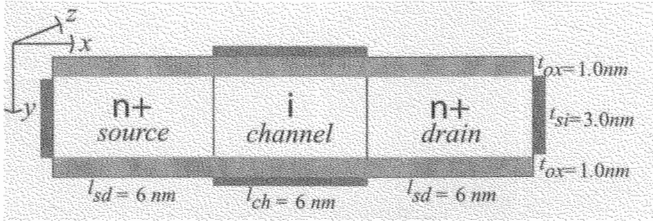
Fig. 2   Schematic cross section view of the double-gate MOSFET under simulation. It has an intrinsic Si channel and the source/drain is doped at 1×10^{26} m^{-3}, respectively. The channel region is controlled by two symmetrical gates at top and bottom. The oxide thickness is 1.0 nm for both top and bottom gates and the silicon thickness is 3.0 nm.
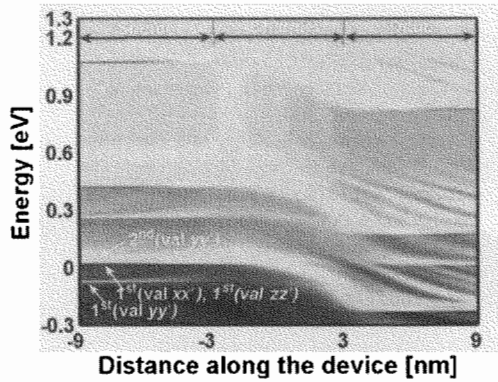

Fig. 3   Local density of states of the simulated double-gate MOSFET at $V_{GS} = 0.4$ and $V_{DS} = 0.25$ V. 1st and 2nd indicate the number of subbands from all considered valleys. (valleys xx', yy' and zz')
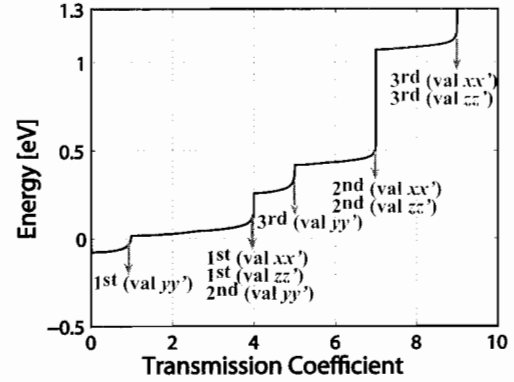

Fig. 4   Plot of transmission versus energy of the simulated double-gate MOSFET at $V_{GS} = 0.4$ and $V_{DS} = 0.25$ V. 1st, 2nd and 3rd indicate 3 subbands are taken into account for all considered valleys. (valleys xx', yy' and zz')
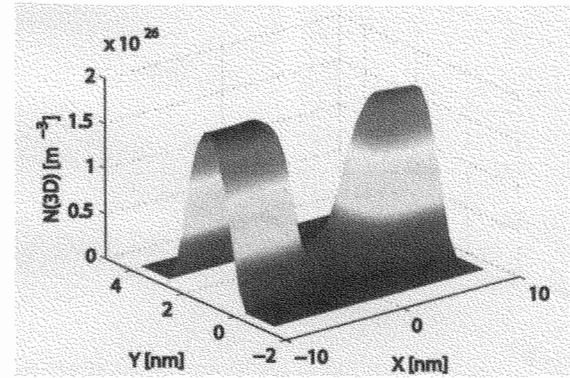

Fig. 5   3D carrier density profile in x-y cross section of the simulated double-gate MOSFET at $V_{GS} = 0.4$ and $V_{DS} = 0.25$ V.
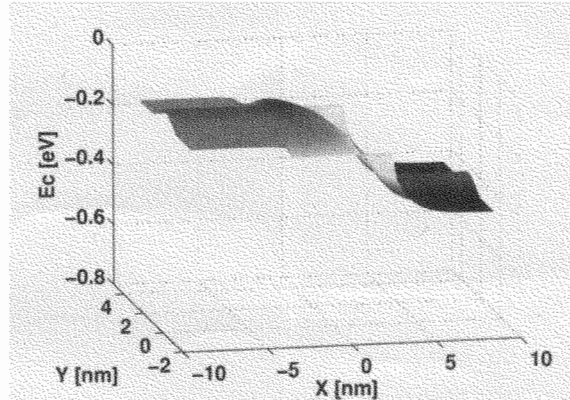

Fig. 6   Conduction band edge profile in x-y cross section of the simulated double-gate MOSFET calculated at $V_{GS} = 0.4$ and $V_{DS} = 0.25$ V.

valleys have lighter effective mass in the direction of applied field. In the simulation, source-to-drain biases of 0 to 0.25 V and gate biases of 0, 0.1 V and 0.4 are used.

The quantum transport modeling is performed by solving a 2-D Poisson equation self-consistently coupled with mode space 1-D transport model [12]. The mode space solution has shown good agreement with 2D transport model and efficient for modeling electron transport in nanoscale silicon-on-insulator (SOI) MOSFETs [25]. In the simulations, we have chosen 3 subbands (modes) which is sufficient for 3.0 nm channel thickness as shown in Figs. 3 and 4 where local density of states and transmission are plotted as a contribution from 3 subbands from all considered valleys (valleys xx', yy' and zz'). As observed in Fig. 3, carriers flow not only in the lowest and second subbands of the valley xx' but also from the the first subband of valleys yy' and zz' which have light effective masses in the transport direction and heavy effective masses in the transverse direction.

By summing all quantities from all subbands and all valleys we can obtain total carrier density and potential energy profiles in x-y cross-section of the simulated MOSFET device as plotted in Figs. 5 and 6. Both profiles are calculated by multiband Green's function self-consistent with Poisson equation at $V_{DS} = 0.25$ V and $V_{GS} = 0.4$ V. Due to quantum effects the carrier density reduces to zero at the oxide/silicon interfaces.

The comparison of current characteristics of the simulated device between multiband simulation (MB) results and those of effective mass approximation (EMA) is depicted in Fig. 7. Both simulations are calculated with $V_{GS} = 0.1$ V, $V_{GS} = 0.25$ V and $V_{GS} = 0.4$ V at room temperature (300 K). In general, the current increases with the carrier energy for the multiband model due to the differences of energy dispersion relation with that of single band effective mass model and also due to the down shifting the potential profile in MB model to that of EMA model as demonstrated in Fig. 8. The
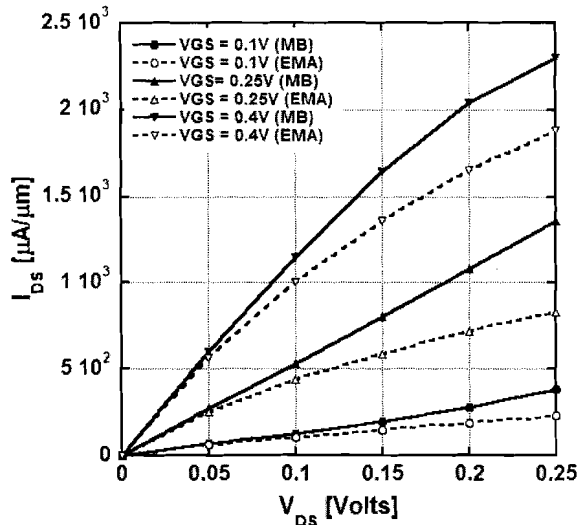
Fig. 7 Drain current versus drain bias, I_{DS} vs. V_{DS}, of the simulated DGMOSFET plotted at 300 K with V_{GS} = 0.1 V, V_{GS} = 0.25 V and V_{GS} = ` V. The solid line is from multiband simulation (MB) and the dash line rom singleband effective mass model (EMA).
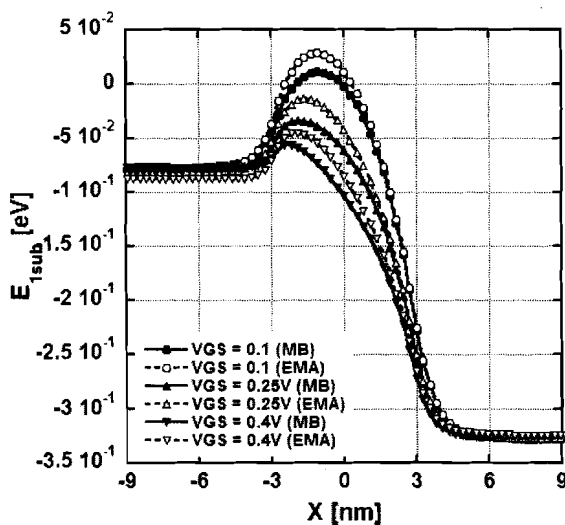
Fig. 8 The first subband energy profiles along the channel of the simulated DGMOSFET plotted at 300 K with V_{GS} = 0.1 V, V_{GS} = 0.25 V and V_{GS} = 0.4 V. The potential profiles of multiband simulation (MB) results is lower than those of singleband effective mass model (EMA).

discrepancy becomes obvious in higher bias because as the bias increases electrons with higher energies tend to contribute to the current.

4. Conclusions

The calculation of quantum electron transport in double-gate MOSFETs based on non-equilibrium Green's function (NEGF) method has been formulated. The realistic bandstructure is realised by tight-binding $sp^3 s^*$ model assuming nearest-neighbor interactions. The effects of non-parabolic bandstructure as well as anisotropic features of Si are studied. Our multiband simulation results in significant dif-

ferences from those of conventional effective mass model where only parabolic singleband is considered in the simulation.

Acknowledgments

References

[1] International Technology Roadmap for Semiconductors 2005 Edition. http://www.itrs.net/reports.html

[2] A.D. Carlo, "Semiconductor nanostructure," Phys. Stat. Sol., vol.217, pp.703–722, 2000.

[3] A.D. Carlo, "Microscopic theory of nanostructured semiconductor devices: Beyond the envelope-function approximation," Semicond. Sci. Technol., vol.18, pp.R1–R31, 2003.

[4] A. Pecchia and A.D. Carlo, "Atomistic theory of transport in organic and inorganic nanostructures," Rep. Prog. Phys., vol.67, pp.1497–1561, 2004.

[5] J.C. Slater and G.F. Koster, "Simplified LCAO method for the periodic potential problem," Phys. Rev., vol.94, pp.1498–1524, 1954.

[6] P. Vogl, H.P. Hjalmarson, and H.D. Dow, "A semi-empirical tight-binding theory of the electronic structure of semiconductors," J. Phys. Chem. Solids, vol.44, pp.365–378, 1983.

[7] G. Klimeck, R.C. Bowen, T.B. Boykin, C. Salazar-Lazaro, T.A. Cwik, and A. Stoica, "Si tight-binding parameters from genetic algorithm fitting," Superlattices Microstruct., vol.27, pp.77–88, 2000.

[8] Y.C. Chang, "Complex band structures of zinc-blende materials," Phys. Rev. B., vol.25, pp.605–619, 1982.

[9] D.J.Y. Ting, T. Yu, and T.C. McGill, "Multiband treatment of quantum transport in interband tunnel devices," Phys. Rev. B., vol.45, pp.3582–3592, 1992.

[10] J.-H. Rhew, Z. Ren, and M.S. Lundstrom, "A numerical study of ballistic transport in a nanoscale MOSFET," Solid State Electron., vol.46, pp.1899–1906, 2002.

[11] A. Svizhenko, M.P. Anantram, T.R. Govindan, B. Biegel, and R. Venugopal, "Two-dimensional quantum mechanical modeling of nanotransistors," J. Appl. Phys., vol.91, pp.2343–2354, 2002.

[12] R. Venugogopal, Z. Ren, S. Datta, and M.S. Lundstrom, "Simulation quantum transport in nanoscale transistors: Real versus mode-space approaches," J. Appl. Phys., vol.92, pp.3730–3739, 2002.

[13] Z. Ren, R. Venugogopal, S. Goasguen, S. Datta, and M.S. Lundstrom, "NanoMOS 2.5: A two-dimensional simulator for quantum transport in double-gate MOSFETs," IEEE Trans. Electron Devices, vol.50, no.9, pp.1914–1925, 2003.

[14] A. Rahman, J. Guo, S. Datta, and M.S. Lundstrom, "Theory of ballistic nanotransistors," IEEE Trans. Electron Devices, vol.50, no.9, pp.1853–1864, 2003.

[15] V.A. Sverdlov, T.J. Walls, and K.K. Likharev, "Nanoscale silicon MOSFETs: A theoretical study," IEEE Trans. Electron Devices, vol.50, no.9, pp.1926–1933, 2003.

[16] J. Wang, P.M. Solomon, and M.S. Lundstrom, "A general approach for the performance assessment of nanoscale silicon FETs," IEEE Trans. Electron Devices, vol.51, no.9, pp.1366–1370, 2004.

[17] M. Bescond, J.L. Autran, D. Munteanu, and M. Lannoo, "Atomic-scale modeling of double-gate MOSFETs using a tight-binding Green's function formalism," Solid State Electron., vol.48, pp.567–574, 2004.

[18] S. Datta, "Nanoscale device modeling: The Green's function method," Superlattices Microstruct., vol.28, pp.253–278, 2000.

[19] S. Datta, Quantum Transport: Atom to Transistor, Cambridge Univ.

Press, Cambridge. U.K. 2005.

[20] M. Ogawa, T. Sugano, and T. Miyoshi, "Mulitband quantum transport with Γ-X valley-mixing via evanescent states," Solid State Electron., vol.42, pp.1527–1532, 1998.

[21] M. Ogawa, T. Sugano, and T. Miyoshi, "Full mulitband simulation of quantum electron transport in resonant tunneling devices," Solid State Electron., vol.44, pp.1939–1947, 2000.

[22] H. Fitriawan, S. Souma, M. Ogawa, and T. Miyoshi, "Multiband simulation of quantum electron transport in nano-scale devices based on non-equilibrium Green's function," SSDM 2006, ed. H. Sakaki, pp.516–517, 2006.

[23] J.A. Stvneng and P. Lipavsky, "Multiband tight-binding approach to tunneling in semiconductor heterostructures: Application to ΓX transfer in GaAs," Phys. Rev. B., vol.49, pp.16494–16504, 1994.

[24] R. Lake, G. Klimeck, R.C. Brown, and D. Jovanovic, "Single and multi-band modeling of quantum electron transport through layered semiconductor devices," J. Appl. Phys., vol.81, pp.7845–7869, 1997.

[25] M. Ogawa, N. Kagotani, M. Ohtani, and T. Miyoshi, "Quantum mechanical simulation in DG MOSFETs based on a tight binding green's function formalism," SISPAD 2004, ed. G. Wachutka and G. Schrag, pp.137–140, Springer, 2004.

Helmy Fitriawan received the B.Eng. in Electronics Engineering from Institute of Technology Bandung, Indonesia, in 1998 and M.Sc. in Data Communications from University of Sheffield, UK, in 2000. From 2000 to 2004, he was a lecturer at the Department of Electrical Engineering, Lampung University, Indonesia. He is currently pursuing Ph.D. degree in Graduate School of Science and Technology, Kobe University. He is a member of the IEEE and the Japan Society of Applied Physics.

Matsuto Ogawa received the B.E. degree from the Department of Electronics Engineering, the University of Tokyo in 1980, M.S. and Ph.D. from there in 1982 and 1985, respectively. In that year he became a research associate at the Department of Electronics Engineering, Kobe University, where he is now a professor. From 1992 to the end 1993, he was on leave at IBM T.J. Watson Research Center in New York as a visiting Scientist. He has been engaged in research on quantum devices and opto-electronics. He is a member of the IEEE and the Japan Society of Applied Physics. He received an Outstanding Achievement Award for a pioneering research on nanoscale device simulator in 2006 from the Institute of Electronics, Information and Communication Engineers of Japan.

Satofumi Souma received his B.S., M.S., and Ph.D. degrees from the Department of Physics, Tokyo University of Science, Japan, in 1994, 1997, and 2000, respectively. From 2001 to 2003, he was with the Quantum-functional Semiconductor Research Center, Dongguk University, South Korea, first as a postdoctoral research fellow and later as a research professor. In 2003, he joined the Quantum Transport Theory Group in the Department of Physics, University of Delaware, USA, where he was a postdoctoral research fellow until March 2005. Then he moved to the Department of Physics, Tokyo University of Science, Japan, as a researcher supported by the CREST project of Japan Science and Technology Agency. In April 2006, he joined the Department of Electrical Engineering, Kobe University, where he is currently a research associate. He is a member of the Physical Society of Japan and the American Physical Society.

Tanroku Miyoshi received the B.S. in electrical engineering from the University of Tokyo, Tokyo, Japan, in 1967, and the M.S. and Ph.D. degrees in electronic engineering from the University of Tokyo, Tokyo, Japan, in 1969 and 1972, respectively. In 1972 he was appointed lecturer, and from 1974 to 1987, he was an associate professor in the Department of Electronic Engineering, Kobe University, Kobe, Japan, where he is presently a professor. He has been engaged in research of electromagnetic wave theory, microwave integrated circuits, and lightwave electronics. His current research includes quantum transport modeling in nanostructures. In 1976 he was a visiting scholar at McGill University, Montreal, PQ, Canada. From 1982 to 1984, he was a visiting scientist at Bell Laboratories, Holmdel, NJ, U.S.A. He is a member of the IEEE, the Japan Society of Applied Physics, and the Japan Society for Simulation Technology. He received Yonezawa Award in 1974, Outstanding Book Award in 1977, and Electronics Society Award in 2006 from the Institute of Electronics, Information and Communication Engineers of Japan.